# Plasmon guided modes in nanoparticle metamaterials

**R. Sainidou and F. J. García de Abajo***

*Instituto de Óptica - CSIC, Serrano 121, 28006 Madrid, Spain*
**Corresponding author: jga@cfmac.csic.es*

**Abstract:** Surface modes in nanostructured metallic metamaterial films are reported showing larger confinement than plasmons in metallic waveguides of similar dimensions, but in contrast to plasmons, the new modes have TE polarization. The metamaterial, formed by planar arrays of nearly-touching metallic nanoparticles, behaves as a high-index dielectric for the noted polarization, thus yielding well confined guided modes. Our results for silver particles in silica support a new paradigm for TE surface-wave guiding in unconnected nanostructured metallic systems complementary to TM plasmon waves in continuous metal surfaces.



**OCIS codes:** (240.6690) Surface waves; (160.3918) Metamaterials; (240.6680) Surface plasmons; (160.4236) Nanomaterials.

## References and links

1. G. T. Reed and A. P. Knights, *Silicon Photonics: An Introduction* (Wiley, New York, 2004).
2. D. Sarid, "Long-range surface-plasma waves on very thin metal films," Phys. Rev. Lett. **47**, 1927–1930 (1981).
3. P. Berini, Phys. Rev. B **61**, 10484 (2000); **63**, 125417 (2001).
4. H. T. Miyazaki and Y. Kurokawa, "Squeezing visible light waves into a 3-nm-thick and 55-nm-long plasmon cavity," Phys. Rev. Lett. **96**, 097,401 (2006).
5. R. Ulrich and M. Tacke, "Submillimeter waveguiding on periodic metal structure," Appl. Phys. Lett. **22**, 251–253 (1972).
6. A. P. Hibbins, B. R. Evans, and J. R. Sambles, "Experimental verification of designer surface plasmons," Science **308**, 670–672 (2005).
7. J. B. Pendry, L. Martín-Moreno, and F. J. García-Vidal, "Mimicking surface plasmons with structured surfaces," Science **305**, 847–848 (2004).
8. F. J. García de Abajo and J. J. Sáenz, "Electromagnetic surface modes in structured perfect-conductor surfaces," Phys. Rev. Lett. **95**, 233,901 (2005).
9. F. J. García de Abajo, "Light scattering by particle and hole arrays," Rev. Mod. Phys. **79**, 1267–1290 (2007).
10. In virtue of Babinet's principle, the modes of an array of perfectly-conducting coplanar disks have rigorously the same dispersion relation as the modes of the complementary hole array.
11. N. Stefanou, V. Yannopapas, and A. Modinos, Comput. Phys. Commun. **113**, 49 (1998); **132**, 189 (2000).
12. D. R. McKenzie and R. C. McPhedran, "Exact modelling of cubic lattice permittivity and conductivity," Nature **265**, 128–129 (1977).
13. J. T. Shen, P. B. Catrysse, and S. Fan, "Mechanism for designing metallic metamaterials with a high index of refraction," Phys. Rev. Lett. **94**, 197,401 (2005).
14. S. Riikonen, I. Romero, and F. J. García de Abajo, "Plasmon tunability in metallodielectric metamaterials," Phys. Rev. B **71**, 235,104 (2005).
15. P. B. Johnson and R. W. Christy, "Optical constants of the noble metals," Phys. Rev. B **6**, 4370–4379 (1972).
16. I. Romero, J. Aizpurua, G. W. Bryant, and F. J. García de Abajo, "Plasmons in nearly touching metallic nanoparticles: Singular response in the limit of touching dimers," Opt. Express **14**, 9988–9999 (2006).
17. J. R. Krenn, A. Dereux, J. C. Weeber, E. Bourillot, Y. Lacroute, J. P. Goudonnet, G. Schider, W. Gotschy, A. Leitner, F. R. Aussenegg, and C. Girard, "Squeezing the optical near-field zone by plasmon coupling of metallic nanoparticles," Phys. Rev. Lett. **82**, 2590–2593 (1999).
18. S. A. Maier, P. G. Kik, H. A. Atwater, S. Meltzer, E. Harel, B. E. Koel, and A. A. G. Requicha, "Local detection of electromagnetic energy transport below the diffraction limit in metal nanoparticle plasmon waveguides," Nat. Mater. **2**, 229–232 (2003).

#91590 - $15.00 USD
Received 10 Jan 2008; accepted 19 Feb 2008; published 18 Mar 2008

19. R. Zia, J. A. Schuller, A. Chandran, and M. L. Brongersma, "Plasmonics: The next chip-scale technology," Mater. Today **9**, 20–27 (2006).
20. To a first-order approximation, the trapping coefficients of Figs. 1(b) and 1(f) can be added to describe particle arrays lying on a plasmon-supporting metal rather than a perfect conductor.

## 1. Introduction

Optical signals encoded in light surface waves present numerous advantages over electrical signals, and in particular the larger bandwidth resulting from simultaneously using multiple frequencies, together with the high degree of integration that can be achieved when metallic components are employed. In this context, silicon-on-silica technology allows waveguiding in 300-nm silicon films with negligible absorption losses [1], while metal films narrowed down to tens of nanometers can host long-range surface-plasmon polaritons (SPPs) [2] that persist in laterally confined metallic waveguides [3]. In a recent development, record levels of mode confinement have been achieved in metal-insulator-metal structures at the expense of reducing the propagation length [4].

Surface electromagnetic waves have also been known for some time to exist in textured perfect conductors, and particularly in metallic films [5, 6] and semi-infinite metals [7] pierced by subwavelength hole arrays. These modes are well understood in terms of the self-consistent interaction between the dipoles induced in the small holes [8]. Furthermore, Babinet's principle for thin-film hole arrays permits establishing the existence of similar modes in the complementary particle arrays [9, 10].

Some of these configurations are succinctly described in Fig. 1. Modes in planar structures are naturally described by an $\exp(\mathrm{i}\mathbf{k}_{\parallel}\cdot\mathbf{R})$ dependence on the lateral coordinate vector $\mathbf{R}$, where $\mathbf{k}_{\parallel}$ is the component of the wavevector parallel to the surface. In particular, confined surface waves must have $k_{\parallel}=k(1+\gamma)>k$, where $k$ is the light wavevector in the surrounding semi-infinite medium and $\gamma$ is a trapping coefficient that determines the extension of the field away from the plane $d_{\perp}$ [Fig. 1(a)]. For instance, SPPs decay evanescently on both sides of a metal-dielectric interface [Fig. 1(b)]. Similarly, dielectric waveguide films can sustain modes of TE and TM polarization with no cutoff in wavelength relative to film thickness $d$ [Fig. 1(c)]. Actually, TE modes are highly confined for large permittivity $\varepsilon$. Both polarizations are also possible in particle arrays, with the degree of planar trapping increasing with the inverse of the area per particle ($1/A$) and the particle polarizability $\alpha_{\parallel}$, $\alpha_{\perp}>0$ along directions parallel and perpendicular to the plane of the array, respectively [Fig. 1(e)].

In this paper, we demonstrate a hybrid between the structures of Figs. 1(c) and (e), whereby a planar array of particles in the nearly-touching limit behaves as a dielectric film of large effective refraction index capable of hosting TE waves. These surface waves, which are generally occurring in unconnected metallic networks, are more confined than SPPs in metallic films of identical thickness, and therefore they are complementary to SPPs of TM polarization showing up in continuous metallic surfaces. In both cases, the trapping is enhanced through structuring. Furthermore, these surface waves are highly tunable by varying the size and separation of the particles. All our reported calculations are obtained by rigorous solution of Maxwell's equations using a layer-Korringa-Kohn-Rostoker procedure [11].

## 2. High-index nanoparticle metamaterials

The permittivity of dielectrics in the visible and near-infrared (vis-NIR) spectral region is limited to values $<16$ in naturally occurring materials (e.g., Ge and Si), but certain engineered metamaterial designs are known to exhibit large effective dielectric constant [12, 13]. In particular, arrays of perfectly-conducting spheres in the nearly-touching limit behave as artificial dielectrics of effective permittivity $\varepsilon_{\mathrm{eff}}$ diverging in the nearly-touching limit [12] [Fig. 2(a)],

#91590 - $15.00 USD Received 10 Jan 2008; accepted 19 Feb 2008; published 18 Mar 2008

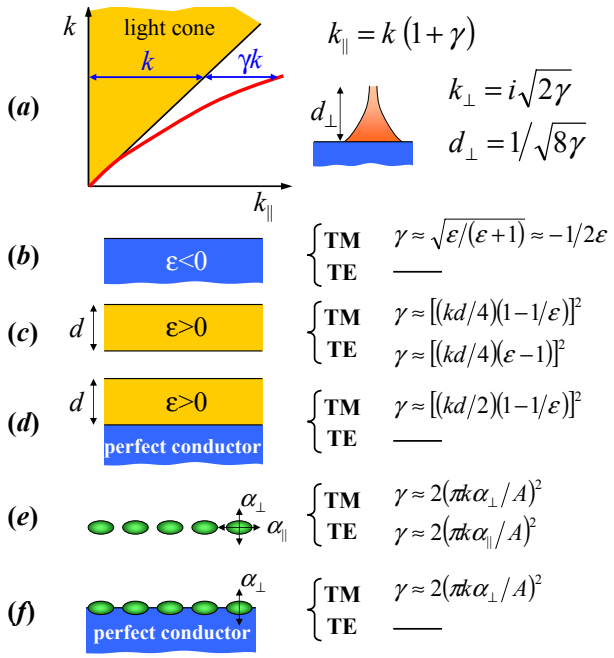


Fig. 1. **(a)** Surface electromagnetic waves are characterized by a surface component of their wavevector ($k_{\|}$) exceeding the momentum in the surrounding medium ($k$) and they pop up evanescently away from the surface up to a distance $d_\perp$ that decreases with increasing trapping coefficient $\gamma$. **(b)-(f)** Various forms of light confinement at surfaces: (b) surface-plasmon polaritons, (c) dielectric waveguides, (d) supported dielectric waveguides, (e) planar particle arrays in a symmetric environment ($A$ is the area per particle and $\alpha$ the polarizability), and (f) particle arrays supported on metal. The trapping coefficient $\gamma$ is given in the limit of large $\varepsilon$ in (b), small thickness $d$ in (c) and (d), and small particles in (e) and (f), both for TM and TE modes. Notice that $\alpha_{\|}, \alpha_\perp > 0$ is required in (e) and (f) for the existence of the modes [9].

and with significant magnetic response depending on the value of the skin depth relative to the diameter $D$ (see below). An effective permittivity description is of course only appropriate in the long wavelength limit (i.e., for $\lambda \gg D$). At vis-NIR wavelengths, this means that the metamaterial must be formed by nanoparticles, the optical response of which contains plasmons and other non-perfect-metal characteristics. This is analyzed in Fig. 2(b) for silver spheres surrounded by silica and for several values of the metal filling fraction.

We derive effective optical constants by comparing the reflection coefficients of semi-infinite particle arrangements to Fresnel's formulas for equivalent homogeneous media [14]. The effective permittivity approaches the perfect-conductor limit at long wavelengths, but increases significantly at larger frequencies due to polarization of nanoparticle plasmon resonances lying in the visible (i.e., this increase is produced by the long-wavelength tail of those plasmon modes, involving the entire metamaterial). Values of $\varepsilon_{\text{eff}} > 40$ are predicted for instance at $\lambda = 1000$ nm for particles of 100 nm diameter separated by gaps of 2 nm.

The origin of these effects can be traced back to the electric-field enhancement in the gap regions of neighboring spheres for external electric-field components perpendicular to the interparticle gaps [16]. The space-averaged electric field can be substantially larger than the applied field, thus yielding high values of the effective permittivity. A similar effect has been predicted

#91590 - $15.00 USD
Received 10 Jan 2008; accepted 19 Feb 2008; published 18 Mar 2008

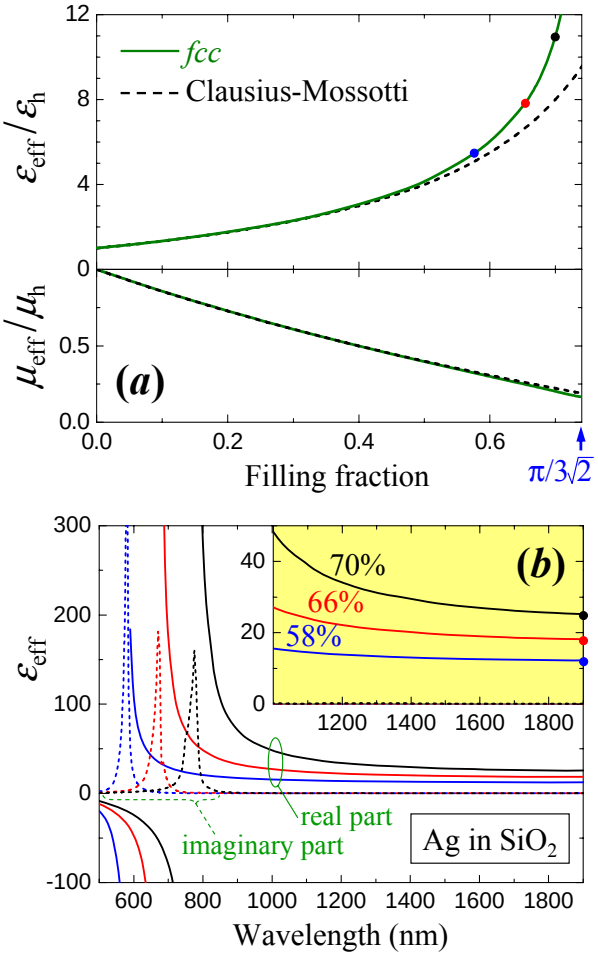


Fig. 2. **(a)** Effective electrostatic dielectric constant $\varepsilon_{\rm eff}$ and magnetostatic magnetic permeability $\mu_{\rm eff}$ of a *fcc* array of perfect-conductor spheres as a function of the filling fraction of the metal up to the *fcc* nearly-touching limit. The spheres are embedded in a homogeneous host medium of permittivity $\varepsilon_h$ and permeability $\mu_h$. Rigorous electromagnetic calculations (solid curves) are compared to the Clausius-Mossotti relation (broken curves). **(b)** Vis-NIR effective permittivity of *fcc* arrangements of silver spheres embedded in silica for three different values of the metal filling fraction. The inset shows a magnification of the long-wavelength tails. The complex spectral dependence of the dielectric constant of silver and silica is taken from optical data [15].

#91590 - $15.00 USD
Received 10 Jan 2008; accepted 19 Feb 2008; published 18 Mar 2008

in slit arrays cut in perfect-conductor films [13].

It should be mentioned that the perfect-conductor granulate metamaterials of Fig. 2(a) exhibit a significant magnetic response ($\mu \neq \mu_h$), but this point deserved further clarification: this magnetic response occurs when the skin depth $\delta$ is small compared to the particle diameter ($\delta \ll D \ll \lambda$), due to the exclusion of magnetic field from the metal. Actually, the magnetic dipolar polarizability of $|\varepsilon| = \infty$ spheres, given by $\alpha_M = -D^3/16$ in the $\delta \ll D$ limit, is significant compared with the electric polarizability $\alpha_E = D^3/8$. In contrast, the $D \ll \delta \ll \lambda$ limit yields $\alpha_M = 0$ and the metamaterial has $\mu = \mu_h$.

## 3. TE surface modes in a closely-packed monolayer of nanoparticles

A single layer of closely-packed metallic particles is sufficient to have the field along inter-particle gaps and produce the desired effect of large $\varepsilon_{\text{eff}}$ when TE polarization is considered. Therefore highly-confined modes similar to those of a high-index dielectric film are expected to exist in particle monolayer arrangements.

We show in Fig. 3 a particular example of this behavior for a hexagonal array of 100-nm silver particles embedded in silica and with 4.17 nm spacing between particle surfaces. The predicted TE surface waves [black solid curve in Fig. 3(a)] lies much further away from the light cone compared to SPPs in a silver-silica interface (dashed curve; SPPs in 100-nm thick film have nearly the same dispersion relation as the semi-infinite metal on the scale of the figure). Actually, we obtain TE waves with similar dispersion relation in a homogeneous 100-nm thick dielectric film of $\varepsilon_{\text{eff}} = 19$ (dotted curve), which compares very well with the value of $\varepsilon_{\text{eff}}$ obtained for bulk *fcc* particle arrangements of the same metal filling fraction [see 66% curve in the inset of Fig. 2(b)]. The displayed surface wave of the array is in fact the lower-order mode of a series that includes a rich structure of TE and TM waves, some of them exhibiting zero and negative group velocity over a wide range of parallel momenta. A sample of this behavior is shown in the first two higher-order modes of Fig. 3(a) (gray solid curves). These modes have TE symmetry as well, while TM modes are also supported, but are much closer to the light line, as expected from Fig. 1(c).

In contrast to mode propagation in linear nanoparticle arrays [17, 18], our modes rely on the availability of inter-particle directions perpendicular to the mode propagation direction, and therefore, the physics in our structure is of a fundamentally different nature. We realize this condition in planar particle arrays, but similar results should be observed as well in linear arrays if each particle is replaced by nearly-touching dimers oriented perpendicular to the linear chain direction. However, these modes cannot exist in single linear arrays.

The propagation distance in the particle array of Fig. 3(a) [see Fig. 3(b)] is reasonably large (e.g., 15 $\mu$m at $\lambda = 1550$ nm), although substantially shorter than SPPs in a silver-silica interface (400 $\mu$m at the same wavelength). This decrease in propagation length is generally associated to stronger confinement [4] because the mode field intensity has more weight in the absorbing metallic part of the structure. This effect is amplified by the lower group velocity of the surface waves in the particle array, which take longer to propagate along a given distance. It should also be noticed that the periodicity of the array prevents radiation losses, although imperfections in the particle array (e.g., inhomogeneous particle size and displacements from lattice positions) can limit propagation through coupling to scattered light.

Figure 3(c) offers a graphical demonstration that the trapping mechanism of our TE surface modes is relying on field enhancement at the inter-particle surfaces perpendicular to the electric field, which in turn produces a large effective permittivity. The contour plots represent the electric field within a plane parallel and close to the sphere array. The arrows show the direction of the parallel wavevector, so that the field is preferentially directed perpendicular to them. The electric-field intensity is small near particle gaps oriented along the parallel wavevector, and

#91590 - $15.00 USD Received 10 Jan 2008; accepted 19 Feb 2008; published 18 Mar 2008

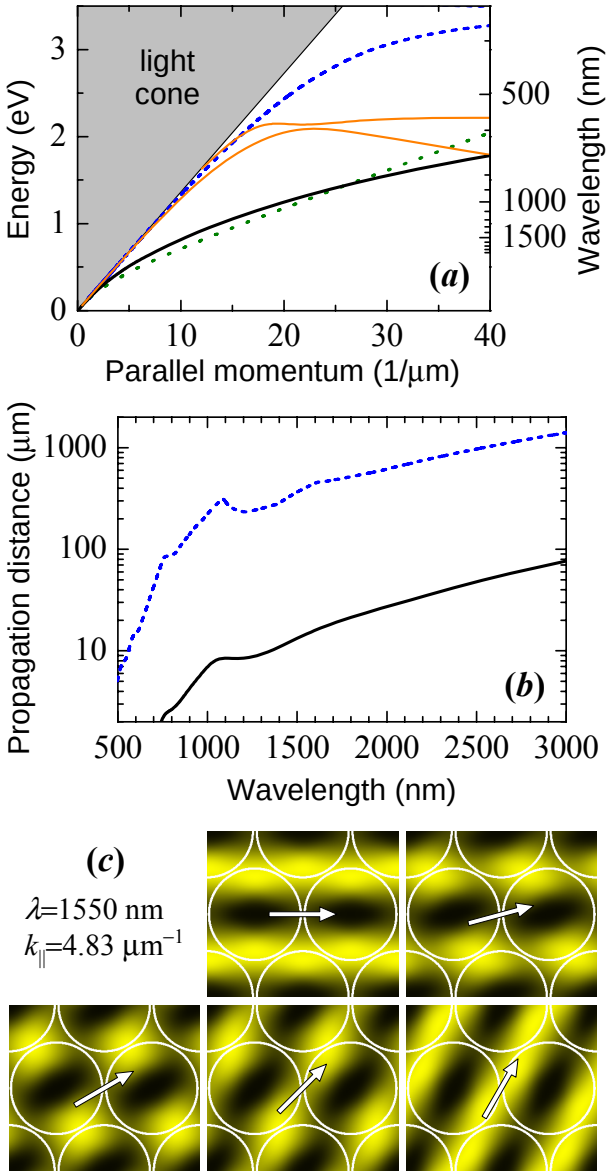


Fig. 3. **(a)** Dispersion relation of the TE mode of a hexagonal layer of 100-nm-diameter silver spheres embedded in silica for a separation between particle surfaces of 4.17 nm (black solid curve). The parallel momentum is directed along a nearest-neighbor vector (ΓK direction) and extends up to the first Brillouin zone boundary. This is compared to the TE mode of a 100-nm-thick dielectric waveguide of $\varepsilon = 19$ material surrounded by silica (dotted curve), and to the surface plasmon polaritons (TM polarization) of a silver-silica planar interface (dashed curve). Higher-order modes of the arrays are also shown (gray solid curves). **(b)** Propagation distance of the particle array and the silver-silica interface considered in (a). **(c)** Electric-field intensity in a plane located 5 nm away from the particle surfaces at the $\lambda = 1550$ nm surface mode for various orientations of the parallel momentum vector relative to the lattice (see arrows) and for $k_{\|} = 4.83\ \mu\text{m}^{-1}$. The intensity scale is linear and the maxima correspond to bright regions.

#91590 - $15.00 USD
Received 10 Jan 2008; accepted 19 Feb 2008; published 18 Mar 2008

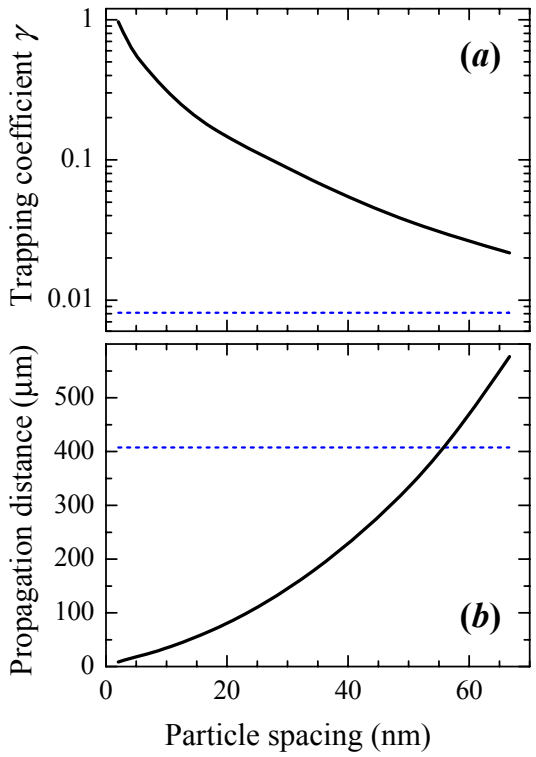


Fig. 4. **(a)** Trapping coefficient of a hexagonal layer of 100-nm-diameter silver spheres in silica as a function of the separation between particle surfaces for a wavelength of 1550 nm. **(b)** Propagation distance of the modes considered in (a). The values corresponding to the planar silver-silica interface are signalled by dashed horizontal lines.

conversely, the field maxima occur at particle gaps with non negligible projection perpendicular to that wavevector.

The dependence of the degree of surface wave confinement on particle separation is illustrated in Fig. 4 for fixed wavelength ($\lambda = 1550$ nm) and particle diameter (100 nm). The trapping coefficient $\gamma$ shows a rapid increase as the particle separation decreases, reflecting the divergence of $\varepsilon_{\text{eff}}$ near the nearly-touching limit in metallic-particle metamaterials [see Fig. 2(a)]. The increase in binding is accompanied by a decrease in propagation distance [Fig. 4(b)]. Interestingly, the TE modes of the particle array can have similar propagation distance as SPPs for separations above 60 nm, but with significantly larger binding.

## 4. Conclusions

With the promise of plasmonics to become the natural high-frequency ($\sim$ 100 THz) substitute of current GHz electronic technology [19] (both requiring sub-micron tailoring of metal components), our predicted, strongly-bound TE surface waves in electrically unconnected particle arrays constitute a powerful extension of SPPs. But there is also room to play with continuous metal films: the parallel electric field is largely quenched in metals, and this is why SPPs have TM polarization in planar metallic surfaces; however, adding subwavelength texture increases the degree of TM-waves confinement through polarization normal to the surface, as illustrated in Fig. 1(f) for particles sitting near a perfect conductor [8, 20].

#91590 - $15.00 USD
Received 10 Jan 2008; accepted 19 Feb 2008; published 18 Mar 2008

In summary, we have demonstrated that closely-packet planar metallic nanoparticle arrays host surface electromagnetic waves in the vis-NIR regime that are more confined than SPPs in metal films of the same thickness. Furthermore, our reported modes are complementary to SPPs because they have opposite polarization (TE) and occur in electrically unconnected systems. These waves, which are natural candidates for optical interconnect applications, open up a broad field of nanoparticle-based waveguiding with completely different premises compared to previous linear-chains studies. The infinite planar array configuration presented here is just a particular example of a vast range of possibilities that are waiting to be explored.

**Acknowledgments**

This work has been supported by the Spanish MEC (NAN2004-08843-C05-05, MAT2007-66050, and *consolider* NanoLight.es) and by the EU-FP6 (NMP4-2006-016881 "SPANS").

#91590 - $15.00 USD Received 10 Jan 2008; accepted 19 Feb 2008; published 18 Mar 2008